CURRENT PATHS DURING VACUUM ARC REMELTING OF ALLOY 718

Rodney L. Williamson and Gregory J. Shelmidine

Liquid Metal Processing Laboratory
Sandia National Laboratories
Albuquerque, New Mexico 87185-1134

Abstract

Measurements of crucible voltage and temperature profiles were made during steady-state vacuum arc remelting of a 0.435 m diameter Alloy 718 electrode into 0.540 m diameter ingot in a coaxial furnace. The results are used to estimate the amount of current passing through the ingot/stool contact zone (I_{is}) and the length of the ingot/wall contact zone (h_{iw}). The estimates of I_{is} varied linearly from ~1000 A to ~800 A over a range of ingot lengths extending from 0.8 to 1.6 m. h_{iw} was determined to be very small, <0.1 m. Additionally, the fraction of current passing through the top ingot surface was estimated to be between 0.5 and 0.8 from the data and physical arguments. This information is required to accurately model the pool shape and fluid flows in the liquid metal pool atop the ingot.

Superalloys 718, 625, 706 and Various Derivatives
Edited by E.A. Loria
TMS (The Minerals, Metals & Materials Society), 2001

Introduction

Successful modeling of the vacuum arc remelting (VAR) process requires knowledge of the electrical current paths in the furnace. With reference to Figure 1, one must know the fraction of the total current that passes through the top ingot surface ($f_{top}=I_{gap}/I_{total}$) as well as the amount of current passing through the ingot/stool (I_{is}) and ingot/wall (I_{iw}) contact zones. It is also important to characterize the area of the ingot/wall contact zone. Without this information, it is impossible to accurately model the pool shape or fluid flows in the pool because the energy distribution in the process is unknown.

In principle, information about the current paths in the furnace may be gained by measuring the voltage distribution along the crucible wall as a function of time relative to some fixed position, say the top of the crucible. Given a coaxial furnace design, the voltage at some position well above the arc zone must be constant, reflecting the total process current passing through the crucible cross section. On the other hand, the voltage at a position well below the arc zone will continuously decrease toward zero as the arc zone moves up the crucible wall with ingot growth. Thus, at a single position on the crucible wall, one expects to see an initial region where the voltage is constant followed by a region where the voltage regularly decreases. There will be an intermediate or transition region where the arc gap is in the vicinity of the voltage probe with significant current passing both below and above it. An idealized voltage history for a single point on the crucible is depicted in Figure 2 where the initial, transition and final regions are labeled 1, 2 and 3. The history is ideal in that it assumes a uniform crucible wall temperature, a single current step associated with the arc gap and ingot/wall contact zone, and constant I_{is}.

Suppose that voltage is continuously measured at several positions along the crucible wall simultaneously. A family of curves will be generated similar to that shown in Figure 2 and a crucible voltage profile can be obtained at any point in time for the section of crucible where the measurements are made. This voltage distribution is related to the current flowing through the crucible wall by the following equation:

$$I(x) = \frac{A}{\rho(x)} \frac{dV}{dx} \qquad (1)$$

where $\rho(x)$ is the position dependent electrical resistivity of the crucible and A is the cross-sectional area of the crucible. Resistivity varies with position because of the temperature distribution along the crucible wall. Thus, by measuring the voltage and temperature distributions along the length of the crucible as a function of time, it is possible to estimate the current distribution as a function of time.

Two major limitations arise when attempting to use Equation 1 to find the current distribution along the crucible. One is that the technique is subject to a great deal of noise because of the derivative term. The second has to do with spatial resolution. For practical reasons, one is limited in the number of thermocouples and voltage probe wires that can be mounted on a crucible, and this causes the spacing between measurement locations to be much larger than the crucible wall thickness, the natural limiting factor for spatial resolution.

This paper reports measurements of the crucible voltage and temperature distributions made during steady-state VAR of a 0.435 m diameter Alloy 718 electrode into 0.540 m diameter ingot at 5800 Amperes of melting current. The measurements were performed at INCO Alloys

International Corp. in Huntington, West Virginia,[1] in a test sponsored by the Specialty Metals Processing Consortium. Equation 1 was used to obtain information about the current distribution along the crucible wall. The data were averaged to address the noise issue. The limitation in spatial resolution was dealt with by a suitable transformation of the data valid under the steady-state assumption.

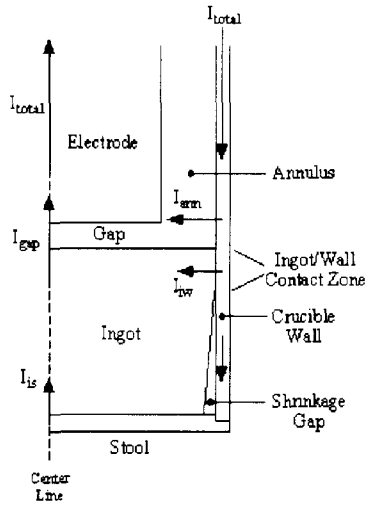

Figure 1. Schematic diagram depicting the current paths in a coaxial VAR furnace.

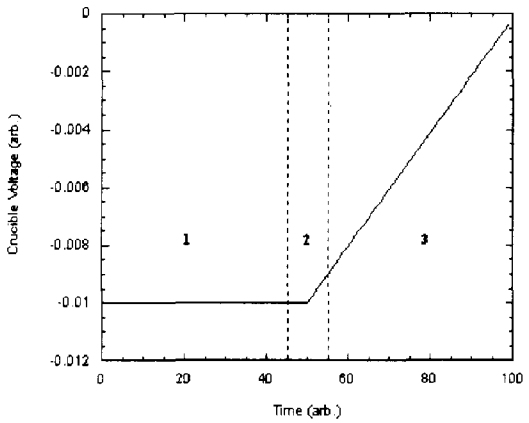

Figure 2. An idealized crucible voltage history.

Experimental Procedures and Methods

One experimental melt was used to acquire the data. The melt parameters were chosen especially for the test and do not represent the standard production practices used by INCO Alloys International Corp.

Voltage probe wires and thermocouples were mounted on a standard VAR crucible as indicated in Figure 3. The wires were mounted by drilling small holes in the side of the crucible, tapping them, and attaching the wires with small machine screws. Type K thermocouples (stainless steel sheaths, ungrounded) were mounted by drilling holes in the crucible so that the hole bottoms were located 7.9 mm (5/16") from the inside surface. To facilitate this, crucible wall thickness measurements were made at the various locations using a calibrated ultrasonic thickness gauge

(Kraut-Kramer-Branson, Model DM2E). Thermocouples were inserted into the holes and "locked" into place by dimpling the material around each hole at several locations with a punch. The wires and thermocouples exited by way of watertight fittings located in two holes drilled through the crucible flange. Each of the voltage probe wires was fed into a high gain (x100), 10 kHz bandpass, isolation amplifier (Analog Devices Mo. 5B40) and the amplifier outputs were recorded on a Metrum Model RSR512 digital tape deck at a 1.25 kHz digitization rate. All voltage measurements were referenced to the same point on the crucible flange. The thermocouple outputs were recorded at 8 Hz on the Metrum tape deck.

Besides the crucible voltage and temperature data, furnace voltage, melting current, pressure, load cell, and melt rate data were acquired from the control room and stored on a second Metrum tape deck. Time was synchronized to within one second on all computers and tape decks. This melt employed helium cooling of the ingot.

Observations and Results

The ingot produced was 2.413 m tall and weighed 4213 kg. Given the average density of the cold ingot, the ingot height as a function of time was estimated from load cell data. Ingot height was crudely corrected for thermal expansion by approximating the thermal distribution in the ingot as linear with a top-to-bottom temperature difference of 1200 °C. A linear thermal expansion coefficient of 1.7×10^{-5} $°C^{-1}$ was used for the correction. This value was calculated from solid density data tabulated in Quested et al..[2] The "corrected" ingot height, h_I, was used in all estimates of pool surface position. The validity of the curve was checked against temperature profile data as described below.

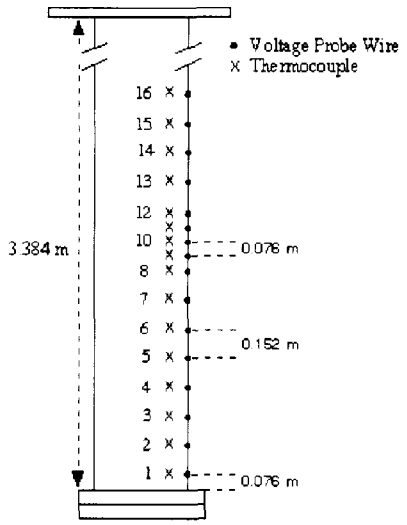

Figure 3. Schematic diagram of the instrumented crucible showing the voltage and temperature measurement locations. All voltages were measured relative to the top flange.

Temperature histories acquired from the thermocouple array are shown in Figure 4. These data were used to generate thermal profiles along the crucible wall for ingot heights in the interval of 0.8 to 2.0 m. A time interval of two hours was chosen for the analysis during which it is assumed that the temperature distribution propagates up the crucible with a constant shape. The ingot grows about 0.25 m in two hours, which corresponds roughly to twice the thermocouple spacing in the low resolution part of the array. Temperature data in each two hour interval were labeled T_{ij} where i refers to time t_i at which the temperature data in row i were acquired and j refers to

the thermocouple number. The center of the time interval was denoted t_0 and is the time about which the transformation was performed. The transformation is given by

$$\Delta x_i = (t_0 - t_i)*u_I \tag{2}$$

where u_I is the average ingot growth rate over the time interval. A position matrix, X, was generated from

$$X_{ij} = x_j + \Delta x_i \tag{3}$$

where x_j is the position of thermocouple j. Under the steady-state assumption, T_{ij} is the temperature that would have been measured at position X_{ij} along the crucible wall if a thermocouple had been located there. The data were spatially averaged after they were transformed to obtain a temperature distribution along the length of the crucible wall with a resolution of 0.01 m.

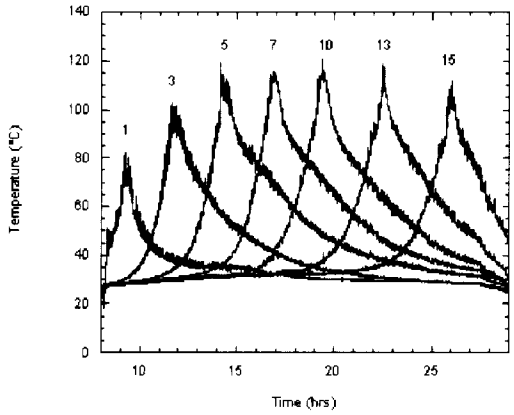

Figure 4. Temperature histories obtained from thermocouples 1, 3, 5, 7, 10, 13, and 15. These thermocouple positions are equally spaced along the crucible. The data have been smoothed over a time period of 1 s.

Figure 5 shows crucible wall temperature profiles generated as described. They are given at one hour intervals starting at t=15:00. The profiles are asymmetric due to heating of the crucible by the upper part of the ingot. This asymmetry becomes worse as the ingot grows causing the peaks to broaden. The data indicate that true steady-state conditions exist only in the region of the arc zone and above, and in the ingot/crucible contact area extending 0.1-0.2 m below the arc zone. However, over a two hour interval the approximation is not too bad and it will be retained for the remainder of the analysis. If the analysis is carried out over one hour intervals, the noise increases but the curve shapes do not change appreciably.

Each temperature profile in Figure 5 peaks at or near the position of the arc zone at the top of the ingot. h_I may be estimated at each of the times for which thermal distributions are shown and plotted as a function of the position at which each curve reaches its maximum temperature value, $x(T_{max})$. The plot is shown in Figure 6. One expects a linear curve with a slope of one if the "corrected" ingot height curve is valid. Linear regression of the data give the following model:

$$h_I = 1.003*x(T_{max}) - 0.0018 \text{ m} \tag{4}$$

with R^2=0.9996 and σ=0.0078. Considering the 0.01 m resolution of the spatial temperature profiles, the model may be considered to have a slope of unity and an intercept of zero. Thus, consistent with expectation, h_1 faithfully tracks $x(T_{max})$, i.e. the positions of the temperature peaks remain constant relative to the pool position. In the calculations carried out below, the random error of h_1 will be set to reflect the standard deviation of the fit of Equation 4, namely ±0.01 m.

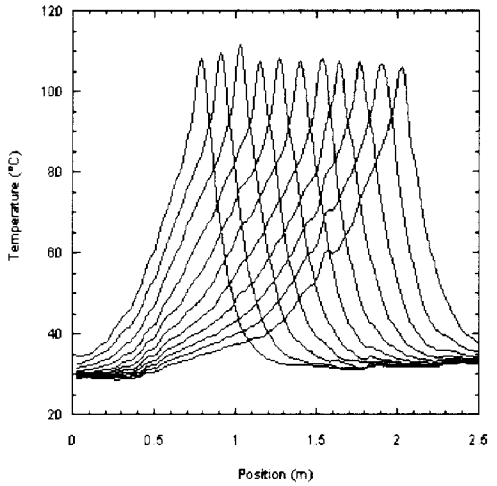

Figure 5. Crucible wall temperature profiles plotted at one hour intervals starting at t=15:00 and ending at t=25:00.

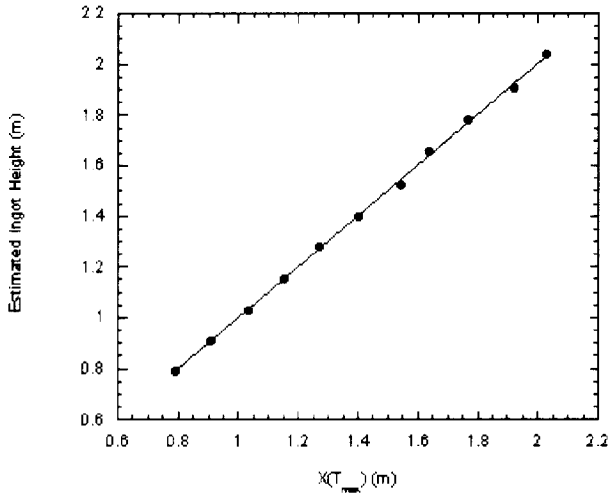

Figure 6. Plot of estimated ingot height as a function of the position of T_{max} in the spatial temperature profiles. The line is a linear regression fit.

The crucible temperature distributions are needed to calculate current distributions from Equation 1. As described above, the thermocouples were mounted ~8 mm from the inside surface and, therefore, the data give the temperature distribution along the crucible at a single depth; no information about the temperature distribution across the crucible wall was collected. For the purposes of calculating the resistivity, it was assumed that the temperature is uniform across the wall at any given height. Resistivity data for pure copper were taken as tabulated in the CRC Handbook of Chemistry and Physics[3] and fit with a second order polynomial in T (in

Kelvin units). This model was then used to estimate a resistivity distribution along the crucible. The error introduced by this procedure gives rise to a bias error in the calculated current ($I \propto \rho^{-1}$). As will be seen below, this error is positive—the resistivity is too small and the calculation overestimates the current. This is readily verified by comparing the calculated current to the measured total current in the region of the crucible above the arc zone where it is known that the total current flows. If the error is not too large, it is assumed that the current distribution may be corrected by multiplying it by a factor to produce the correct value of the total current in this region. This constant is ~0.89 for this analysis.

Several crucible voltage histories are shown in Figure 7. The curves have a shape similar to the idealized curve of Figure 2 except for the initial steep ramps associated with startup. It will be noted that the sloped parts of the curves do not quite overlap demonstrating that some current is flowing through the ingot/stool contact area. Furthermore, careful inspection reveals that the traces are slightly curved upward and grow closer together over time. This indicates that the ingot/stool current decreases with ingot height.

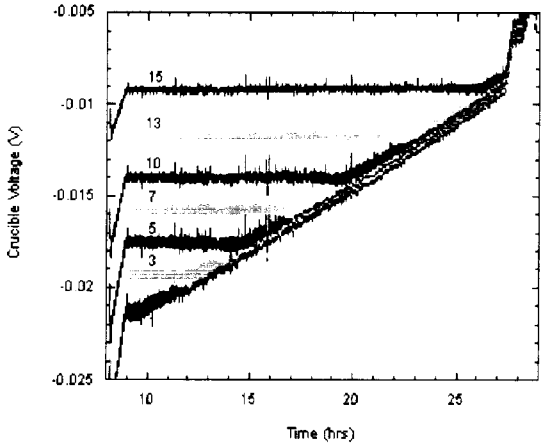

Figure 7. Crucible voltage histories obtained from wires 1, 3, 5, 7, 10, 13, and 15. These wires positions are equally spaced along the crucible. These data have been smoothed over a time period of 1 s.

Crucible voltage profiles can be generated by performing a transformation on the voltage data similar to what was done with the thermocouple data. Figure 8 shows transformed voltage profile data generated at one hour intervals from t=15:00 to t=22:00. Note that the curves above the arc zones overlay as they should: each curve "measures" the total steady-state current. Transforming the curves so that they overlay reveals that the curves diverge a very slight amount below the inflection point. This is due to the non-steady-state character of the thermal profiles below the contact zone as well as differences in I_{is}.

Equation 1 may now be used to generate a current profile from each voltage profile. The simplifying assumption will be made that A is constant and has a value of 0.020 m^2. Voltage noise was diminished by smoothing the data using a running average over a 0.05 m interval before differentiating. This was done based on the assumption that the ingot/wall contact zone proximate to the arc zone is ~0.1 m or larger. A typical result showing profiles with 0.01 m and 0.05 m spatial resolutions is presented in Figure 9 for data centered at t_0=19:00. The vertical dashed line in the figure marks the estimated pool position from which it can be seen that the ingot/wall contact zone (lower shaded area) is very narrow, <0.1 m. The central horizontal

dashed line marks the approximate current at which the pool position intersects the current profile. This constitutes a measure of I_{gap}, ~3300 A. The error in the estimate of I_{gap} is shown by the central shaded region, the width of which reflects the 0.05 m spatial resolution of the more highly smoothed curve. The height was calculated assuming ±400 A uncertainty in the smoothed curve. This gives a value for f_{top} that lies in the range of 0.3 and 0.8, a result that is not particularly useful. This is typical of the values obtained from the other curves.

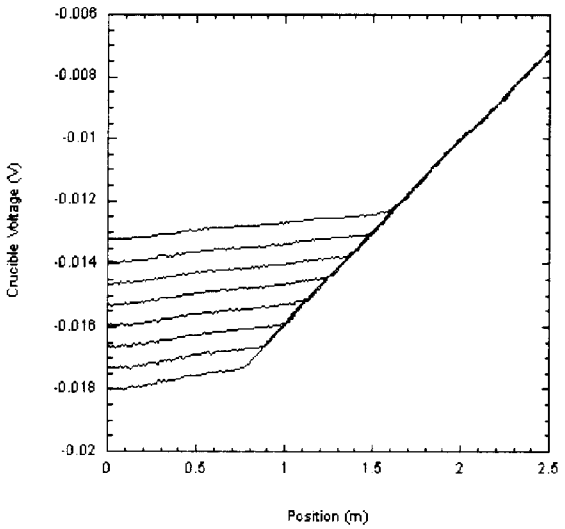

Figure 8. Crucible wall voltage profiles plotted at one hour intervals starting at t=15:00 (lower curve) and ending at 22:00 (upper curve).

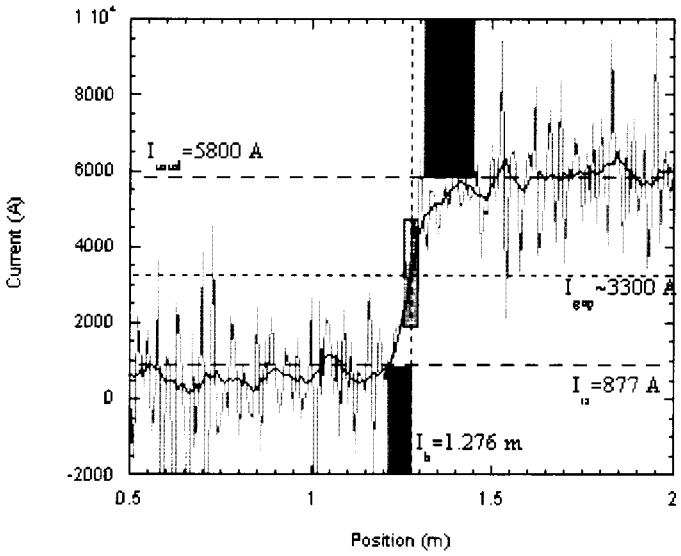

Figure 9. A crucible current profile calculated from Equation 1 from the spatial voltage profile at t=19:00.

Though the curves are very noisy, close inspection of the data reveals a change in slope in the current distribution immediately above the estimated location of the pool surface, dividing the

current conduction into two zones. This observation is made for those profiles generated for times corresponding to when the arc zone was located in the high resolution portion of the voltage probe array. This indicates that the technique is resolving structure in the conduction zone. The primary conduction zone appears to be very narrow. In this region, the current rises very sharply from the stool current to 75 to 85% of the total current. The remaining current is conducted through a region 0.1-0.2 m wide denoted by the upper shaded region in Figure 9. Presumably a third conduction zone might exist in the immediate proximity of the arc gap. However, the height of this zone may be of the same order as the crucible wall thickness and would not be detectable by this measurement technique. Thus, the 75 to 85% of the total current conducted below the diffuse zone may not be a measure of f_{top}, but it does give an estimate of the maximum value possible for f_{top}.

It is apparent from the crucible voltage histories, as well as the crucible voltage profiles, that current was flowing through the stool into the bottom of the ingot throughout the melt. The derived current profiles are too noisy to use for estimation of the ingot/stool current. Instead, the same section of crucible, from 0.10-0.60 m, was chosen over which to evaluate the slope in the voltage distributions shown in Figure 8. The data in this region were fit to straight lines. Stool current was calculated from Equation 1. The calculation at each time should yield a straight, horizontal line: I_{is} should not vary as a function of measurement position. In fact, it varies by about 6% over the range indicating that the calculated resistivity distribution slightly overcorrects the data. The overcorrection improves at later times and is worse at earlier times. A plot of the average, estimated ingot/stool current as a function of ingot height is shown in Figure 10. A linear fit to these data gives a slope of –273 A/m for the dependence of I_{is} on ingot height.

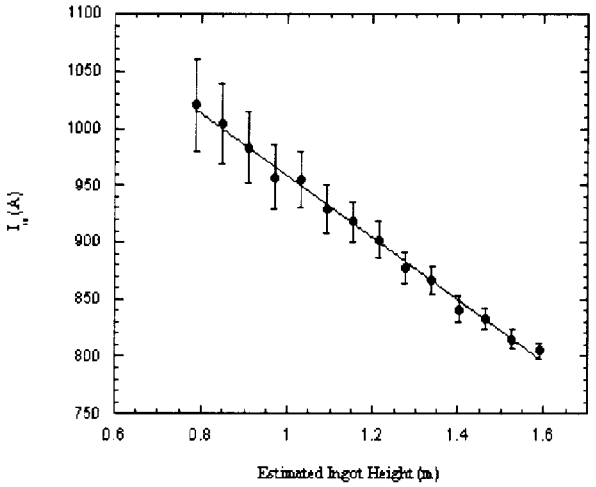

Figure 10. Plot of the average I_{is} as a function of ingot height.

Discussion

Consider the discrete resistance VAR circuit model shown in Figure 11. R_{el} and R_{in} are the electrode and ingot resistances, respectively. The crucible resistance is divided into parts above (R_{cra}) and below (R_{crb}) the arc zone. R_{c1} and R_{c2} are simply circuit resistances due to bus bars, electrical contacts, etc., between the furnace and power supply. $R_{i/s}$, R_{stl} and $R_{s/c}$, are the ingot-stool contact resistance, stool resistance, and stool-crucible contact resistance, respectively. R_{inr} is the radial ingot resistance and $R_{i/w}$ is the ingot-crucible wall contact resistance. R_{gap} and R_{ann}

are the gap and annulus resistances given by the arc plasma resistance to current flow between the anode and cathode. V_c is the cathode fall voltage.

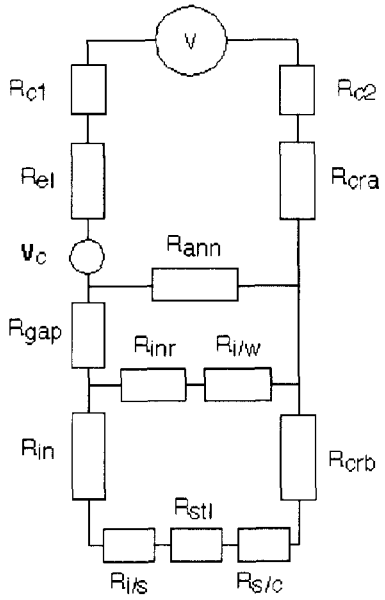

Figure 11. Model VAR furnace circuit.

This circuit model may be analyzed to give expressions for the current conducted between the crucible wall and electrode through the annulus, I_{ann}, through the ingot/crucible wall contact, I_{iw}, and through the ingot/stool contact, I_{is}. They are given by

$$I_{ann} = I_{tot}\left[1 - \frac{R_{ann}}{R_{ann} + R_{gap} + \left(\frac{R_{isc}R_{wall}}{R_{isc} + R_{wall}}\right)}\right] \tag{5}$$

$$I_{iw} = (I_{tot} - I_{ann})\left(\frac{R_{isc}}{R_{isc} + R_{wall}}\right) \tag{6}$$

$$I_{is} = (I_{tot} - I_{ann})\left(1 - \frac{R_{isc}}{R_{isc} + R_{wall}}\right) \tag{7}$$

where the following definitions apply:

$$R_{isc} = R_{in} + R_{stool} + R_{crb} \tag{8}$$

$$R_{stool} = R_{i/s} + R_{stl} + R_{s/c} \tag{9}$$

and

$$R_{wall} = R_{inr} + R_{i/w}. \tag{10}$$

An expression for f_{top} may also be derived. It is

$$f_{top} = \frac{(I_{iw} + I_{is})}{I_{total}} = 1 - \frac{I_{ann}}{I_{total}}$$

$$= \frac{R_{ann}}{R_{ann} + R_{gap} + \left(\frac{R_{isc} R_{wall}}{R_{isc} + R_{wall}} \right)} \tag{11}$$

Equations 5-11 can be used to gain insights into the relative magnitudes of the resistances by simple inspection. Assuming that R_{ann} and R_{gap} are constant throughout the process, variability is introduced into I_{is} (Equation 7) by changes in R_{isc} and R_{wall} (Equations 8 and 10). This assumption is tantamount to asserting constant gap and annulus dimensions, and constant plasma temperature and density. Furthermore, if it is assumed that R_{in} is directly proportional to ingot length but that R_{wall} is relatively unaffected by this parameter, it should be clear that I_{is} will not be a function of ingot length unless R_{in} is larger than, or at least of similar in size to, R_{crb} and R_{stool}. Actually, because the copper wall is cooled and highly conductive, it is probably the lowest resistance in the circuit, implying that

$$R_{in} \approx \text{or} > R_{stool} > R_{crb}. \tag{12}$$

Furthermore, under the additional assumption that the plasma resistances (R_{ann} and R_{gap}) are large compared to the other resistances in the circuit, R_{isc} and R_{wall} must also be of similar magnitude for I_{is} to depend on ingot length. As one might expect from inspection of the circuit, $I_{iw} \rightarrow I_{total} - I_{ann}$ and $I_{is} \rightarrow 0$ as R_{isc} becomes large relative to R_{wall} (Equations 6 and 7). Likewise, if R_{wall} becomes large relative to R_{isc}, the current is shunted completely through the stool and I_{iw} goes to zero (Equation 6). The observation that I_{is} changes by several hundred amperes as the ingot grows indicates that the two lower current paths are somewhat balanced. Thus, an additional relation is

$$R_{wall} \approx R_{isc}. \tag{13}$$

Equation 13 deserves a little more attention. It rests on the additional assumption that the plasma resistances are large compared to the resistances in the lower part of the circuit, namely R_{isc} and R_{wall}. R_{gap} in an Alloy 718 arc has been estimated to be $\sim 10^{-4}$ ohm.[4] Because the annulus gap is typically three to four times as large as the electrode gap and is associated with a smaller surface area of conductor exposed to the region of high plasma density, R_{ann} is expected to be larger than R_{gap} but of the same order of magnitude. On the other hand, R_{isc} is expected to be of the order of the ingot resistance, say 10^{-6} to 10^{-7} ohm, for the reasons given above. Therefore, the decrease in I_{is} with increasing ingot length cannot be due to "extra" current being shunted through the plasma to the wall because the change in R_{isc} is negligible compared to R_{ann}. Instead, this current must be conducted through another leg of the circuit that has a comparable resistance to R_{isc}, namely, through the ingot/crucible wall contact. This is the result expressed by Equation 13. This implies that, in an average way, I_{iw} must be of the same order of magnitude as I_{is}. The average value of I_{is} observed in this study was ~900 A. It might, therefore, be expected that I_{iw} is of this same order of magnitude. This yields 0.3 for a minimum estimate of f_{top} which is right at the lower limit of the experimental value.

The simple circuit model indicates that f_{top} should be independent of ingot height as long as the plasma resistance remains constant. This is seen from Equation 11 by noting that the third term in the denominator is negligible compared to R_{gap} and R_{ann}. Thus, f_{top} is determined by the relative sizes of R_{ann} and R_{gap}. For reasons given above, R_{gap} is expected to be smaller than R_{ann} indicating that f_{top} must be greater than 0.5 under normal melting conditions. This raises the lower limit of expectation by 0.2, yielding an expected value for f_{top} between 0.5 and 0.8. It also emphasizes that f_{top} is expected to be sensitive to electrode gap and annulus spacing, underscoring the importance of good electrode centering practice and effective electrode gap control.

Summary and Conclusions

Measurements of the crucible voltage and temperature histories were made during VAR of a 0.435 m diameter Alloy 718 electrode into 0.540 m diameter ingot at 5800 A of melting current. The data were analyzed to yield temperature and voltage distributions along the crucible at ingot heights between 0.8 and 1.6 m. These were used to gain information about the steady-state current distribution. The following results were obtained:

1) Spatial temperature distributions do not reach steady state below the ingot/wall conduction zone.
2) The ingot/wall conduction zone is very narrow, ~0.1 m or less.
3) I_{is} decreases linearly as a function of ingot height over the range of 0.8 to 1.6 m.
4) f_{top} lies between 0.5 and 0.8 and depends on electrode gap.
5) The conduction zone above the ingot pool surface is ~0.2 m high.

Acknowledgements

A portion of this work was supported by the United States Department of Energy under Contract DE-AC04-94AL85000. Sandia is a multiprogram laboratory operated by Sandia Corporation, a Lockheed Martin Company, for the United States Department of Energy. Additional support was supplied by the Specialty Metals Processing Consortium. The authors also wish to thank INCO Alloys International, Huntington, West Virginia, for hosting the test. Thanks, also, to Lee Bertram of Sandia National Laboratories for helpful suggestions and guidance concerning the data analysis.

References

1. This facility is now owned by Special Metals Corporation.

2. P.N. Quested, K.C. Mills, R.F. Brooks, A.P. Day, R. Taylor, and H. Szelagowski, "Physical Property Measurements for Simulation Modeling of Heat and Fluid Flow during Solidification," *Proceedings of the 1997 International Symposium on Liquid Metal Processing and Casting*, A. Mitchell and P. Auburtin, ed.'s, Santa Fe, NM, February 16-19, 1997, pp. 1-17.

3. 73rd Edition, D. R. Lide, Editor-in-Chief, 1992-1993, p. **12**-34.

4. R. L. Williamson, F. J. Zanner, and S. M. Grose, "Arc Voltage Distribution Properties as a Function of Melting Current, Electrode Gap, and CO Pressure during Vacuum Arc Remelting," *Met. and Mat. Trans. B*, **28B**, 1997, pp. 841-853.